Planning and Execution for Front Delineation and Tracking with Multiple Underwater Vehicles

Andrew Branch[1], Mar M. Flexas[2], Brian Claus[3], Andrew F. Thompson[2], Evan B. Clark[1], Yanwu Zhang[4], James C. Kinsey[3], Steve Chien[1], David M. Fratantoni[5], Brett Hobson[4], Brian Kieft[4], Francisco P. Chavez[4]

[1]Jet Propulsion Laboratory, California Institute of Technology
[2]California Institute of Technology
[3]Woods Hole Oceanographic Institution
[4]Monterey Bay Aquarium Research Institute
[5]Remote Sensing Solutions
Correspondence Author: andrew.branch@jpl.nasa.gov

Abstract

This work describes a planning architecture for a heterogeneous fleet of marine assets as well as a method for detecting and tracking ocean fronts using multiple autonomous underwater vehicles. Multiple vehicles — equally-spaced along the expected frontal boundary — complete near parallel transects orthogonal to the front. Lateral gradients are used to determine the location of the front crossing from each individual vehicle transect by detecting a change in the observed water property. Adaptive control of the vehicles ensure they remain perpendicular to the estimated frontal boundary as it evolves over time. This method was demonstrated in several experiment periods totaling weeks, in and around Monterey Bay, California in May and June of 2017. We discuss the challenges associated with the implementation of the planning system. We show the capability of this method for repeated sampling across a dynamic two-dimensional ocean front using a fleet of three types of platforms: short-range Iver AUVs, Tethys-Class Long-Range AUVs, and Seagliders. This method extends to tracking gradients of different properties using a variety of vehicles.

Introduction

Space-based remote sensing can provide extensive information about ocean dynamics. However, remote sensing information is generally limited to measuring the ocean surface. To probe the ocean interior efficiently requires marine vehicles such as autonomous underwater vehicles (AUVs), gliders, profiling buoys, surface vehicles, and ships sampling in situ. Unfortunately, building, deploying and operating these in situ marine robotic explorers is expensive. As a result, any actual study involves a limited number of marine vehicles, especially when compared to the vast expanse of the ocean. Determining where to deploy and operate marine assets is a challenging problem given the 4D spatiotemporal variations in oceanographic phenomena.

The use of autonomous marine vehicles will increase as the size of ocean observing systems expand in order to study the impact of the oceans on Earth's climate and ecosystems. The day-to-day operations of these systems will become increasingly difficult if human intervention is required. In order to enable large observing systems to operate, techniques for autonomous control of assets based on science goals and data sources such as in situ measurements, remote-sensing, and model-derived data need to be developed. Such observing systems will incorporate a wide variety of vehicles with differing capabilities. Planning and execution systems that leverage existing infrastructure help to reduce the cost associated with the development and maintenance of an observing system as well as maintain flexibility with regards to the planning approach and vehicle availability. The Keck Institute for Space Studies (KISS) Satellites to Seafloor project works towards this goal of fully autonomous sampling [Thompson et al., 2017]. Previous ocean observing systems have relied on substantial human intervention or non-adaptive sampling strategies, including the Autonomous Ocean Sampling Networks (AOSN) [Curtin and Bellingham, 2009; Curtin et al., 1993; Haley et al., 2009; Leonard et al., 2007; Ramp et al., 2009] and the Adaptive Sampling and Prediction (ASAP) [Leonard et al., 2010] projects.

Our project targets automatic generation of coordinated mission plans for teams of assets to follow science derived observation policies (e.g. the use of multiple vehicles to perform transects orthogonal to an ocean front). This paper describes a planning and execution system for a heterogeneous fleet of marine assets. To highlight this system, an approach was developed using multiple vehicles to make a linear estimation of an ocean front's geometry and to continuously direct a team of marine robotic vehicles to perform orthogonal transects with the midpoint of the transect roughly centered on the target front. We describe both the general approach to front-crossing detection, front-geometry estimation, and multi-asset control, the architecture of the planning and execution system for a deployment using three types of vehicles: short-range Iver Autonomous Underwater Vehicles, Long-Range Tethys Autonomous Underwater vehicles, and long-range Seaglider buoyancy driven gliders in Monterey Bay in late spring 2017, the results from the deployment, and the challenges associ-

ated with this system. This deployment was the result of a team effort between the KISS project members and the MBARI Spring 2017 CANON participants [Monterey Bay Aquarium Research Institute, 2017]. The method and systems presented here represent significant steps towards the fully-autonomous adaptive sampling framework as envisioned in Thompson et al. [2017].

Front-Crossing Detection

Lateral Gradient Front-Crossing Detection

The KISS team developed an algorithm to identify a subsurface oceanic front based on lateral gradients of a given hydrographic property. This could be temperature, buoyancy or density (if salinity data is available), or any available biogeochemical property such as dissolved oxygen or chlorophyll.

When in situ data is received in near real time, the algorithm grids the data, smooths it by applying a simple linear weighted average of immediate neighboring measured data points, and calculates the lateral gradients (Figure 1). The algorithm uses temporal gradients, and assumes that time can be linearly related to distance. The algorithm then calculates the lateral gradients along the transect within the layer of interest (defined beforehand by the user) as well as the mean value, and the standard deviation. The user also defines beforehand the number of standard deviations used to declare a front-crossing detection. All points above this threshold are considered potential front crossings (Figure 2). To qualify for a frontal crossing, it is required that the threshold is crossed twice (once entering and once leaving the high gradient region). The width of the front is used to choose the front crossing of interest if more than one is present. The front location, width, and time of crossing is then output for later use in vehicle tasking. An example is shown in Figure 1 and Figure 2. Time, as apposed to distance, is plotted on the x-axis as that is what the algorithm uses. Using real time data from May 4, 2017 (Figure 1d) the algorithm detects five narrow subsurface fronts from 10 to 15 m deep (Figure 2a), and selects the widest front (Figure 2d).

Autonomous Control of Underwater Vehicles for Front Tracking

A technique was developed to control a group of vehicles to repeatedly sample across a dynamic ocean front as it evolves over time. The planner must be able to modify the vehicle transects in order to adapt to the changing ocean conditions. The control algorithm is outlined in Algorithm 1 and shown in Figure 3. The statements in which the planning system interacts with the execution system (i.e. the vehicles) are highlighted. When first deployed, an initial estimated front location and orientation is manually provided based on available data from other assets. The vehicles are equally spaced along this estimated front. Each vehicle is commanded

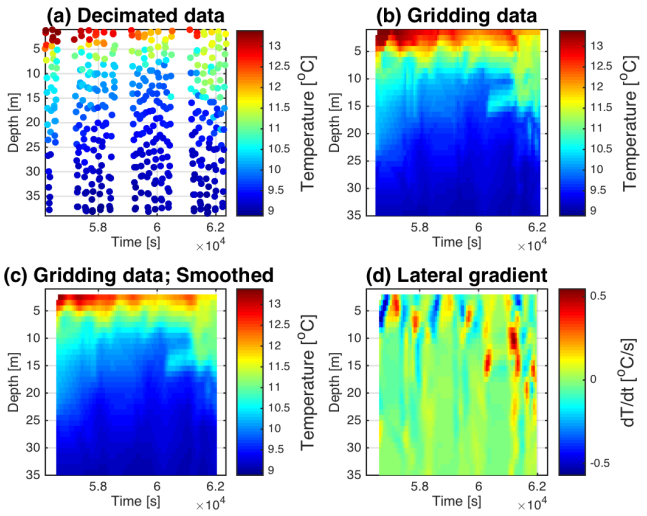

Figure 1: Lateral gradient front-crossing detector. For this example we use data obtained on May 4, 2017 from Iver 136 (segment 000). Real-time in situ temperature data (shown in scatter plot in panel a) is gridded (panel b) and smoothed (panel c). Then, lateral gradients are calculated (panel d). When used in real time, the algorithm uses temporal gradients, and assumes that time can be linearly related to distance.

on an initial transect orthogonal to the estimated front. When the vehicle surfaces to plan, Algorithm 1 is executed. The vehicle location and the scientific data from the current transect are retrieved from the execution system as *vehicle_location* and *transect_data* respectively. The vehicles location along the transect is calculated as $location_p$ by projecting the vehicles current location onto the commanded transect. If the vehicle has traveled a minimum distance along the commanded transect, specified by $transect\_dist_{min}$, then the front-crossing detection algorithm is run on the data from this transect. The resulting front-crossing is defined as $new\_front\_crossing$. If the vehicle is a specified distance past this new front detection, then the front is re-estimated using linear regression on front detections from all vehicles, otherwise the transect is continued. When re-estimating, only certain front detections from each vehicle are considered, specified by $valid\_front\_detections$. We used two methods when selecting the subset of detections used in the linear regression: a time based approach where detections from the last N hours were considered and a latest detection approach where only the last detection from each vehicle was considered. These two approaches are defined in the procedure $get\_estimation\_crossings$. The new $transect_p$ is calculated such that it is orthogonal to $estimated\_front$. The vehicle is then commanded on this new transect. In order to prevent the vehicle from leaving the study area, $transect\_dist_{max}$ is defined. If a transect has reached this length the front is re-estimated, a transect orthogonal to this is defined,

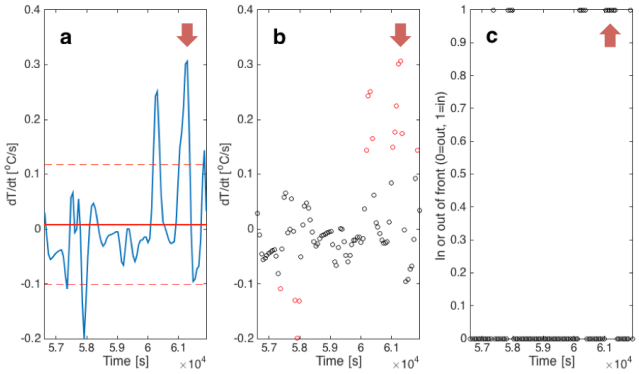

Figure 2: (Continues from Figure 1) The algorithm calculates the mean value of the lateral gradients over the layer of interest. In this example, we use data from 10m to 15m. The algorithm calculates the mean value (bold red line in panel a) and the n-standard deviation (in this case, n=1.2; red broken lines in panel a). All points above the n-value standard deviation are considered potential fronts (red circles in panel b). A boolean is used to isolate the front crossings (panel c). The width of the front is used to choose the front crossing when more than one front is present. The crossing chosen by the algorithm is marked with a red arrow.

and the vehicle is commanded on this new transect.

Pilot Experiment

Experiment Site

The pilot experiment occurred in Monterey Bay, California (36.80°N, 121.90°W) from May to June 2017. The circulation in Monterey Bay is characterized by a persistent coastal upwelling, in response to prevalent northerly winds, which generates highly-productive cold coastal regions [Hickey, 1979; Lynn and Simpson, 1987]. In May 2017, an intensive upwelling plume spread southeastward across the mouth of Monterey Bay. A fleet of AUVs were deployed to detect and track the fronts between the upwelling plume and the stratified inner bay water. Over the shelf, KISS IVERs were set to detect lateral gradients of temperature from 10m to 15m. Over the slope, temperature in the upwelling water column was remarkably homogeneous in the vertical dimension. Over the slope, MBARI LRAUVs were also set to detect lateral gradients of temperatures from 10m to 15m.

Glider retasking took place in June 2017, offshore Point Sur, where the California Undercurrent (CU) becomes unstable [Molemaker, McWilliams, and Dewar, 2015]. Looking for the surface signature of the CU, one Seaglider was set to detect lateral gradients of temperature from 5m to 15m. The operations regions for each vehicle are shown in Figure 4.

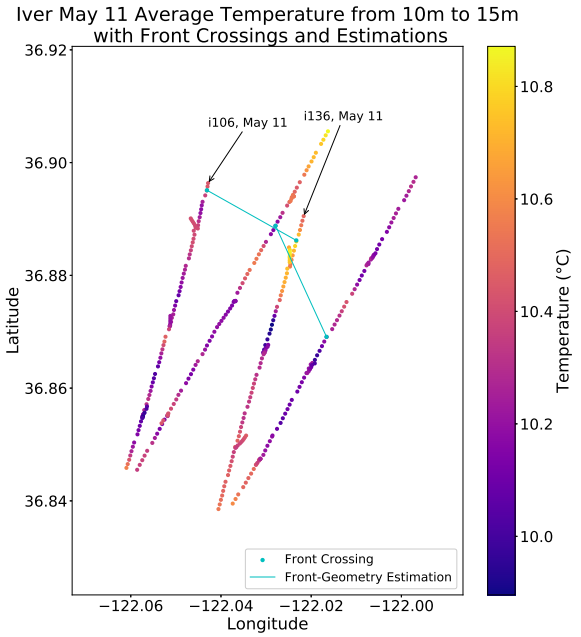

Figure 3: Iver transects on May 11 with temperature averaged from 10 meters to 15 meters plotted. Front crossings are shown as blue dots and estimated fronts are shown as blue lines. Each vehicle starting location is labeled with the vehicle name and the date. The second transect for each vehicle is orthogonal to the estimated front from the front crossings on the first transect.

Instruments

This work was demonstrated across three types of underwater vehicles: the OceanServer Iver AUV, the Kongsberg Underwater Technology, Inc. Seaglider and the MBARI Tethys-class LRAUV (shown in Figure 5). The method is extensible to other platforms and indeed other domains where the vehicles are able to at least intermittently transmit collected data and receive new instructions mid-deployment.

Iver AUVs The highest speed observing platforms used for this field experiment consisted of two Iver2 (Ocean Server Technology Inc.) autonomous underwater vehicles (AUVs) [Crowell, 2006]. Both of the vehicles were equipped with a hull-mounted Neil Brown conductivity/temperature sensor (Ocean Sensors Inc.) which served as the primary scientific payload for this work. Additionally, one of these vehicles, Iver-106, was an Ecomapper variant equipped with a SonTek Doppler velocity log (DVL), an Ocean-Server compass for attitude estimation, a WHOI micro-modem 2 and a depth sensor. The other Iver2 vehicle, Iver-136, was similarly equipped with the WHOI micro-modem 2, compass and depth sensor as well as a dual upward, downward facing 600 kHz RDI phased array DVL, a Microstrain 3DM-

Algorithm 1 Linear Front Delineation and Tracking

procedure VEHICLE_RETASKING ▷ Run this procedure when a vehicle surfaces to plan
  $vehicle\_location \leftarrow$ Get vehicle location
  $transect\_data \leftarrow$ Get vehicle data
  $location_p \leftarrow project\,(transect, vehicle\_location)$
  if $dist\left(transect\_start, location_p\right) >= transect\_dist_{min}$ **then**
    $new\_crossing \leftarrow detect\_crossings\,(transect\_data)$
    if $new\_crossing$ was detected **then**
      $crossings \leftarrow crossings \bigcup \{new\_crossing\}$
      $valid\_crossings \leftarrow get\_estimation\_crossings(crossings)$
      $estimated\_front \leftarrow linear\_regression\,(valid\_crossings)$
      $location_f \leftarrow project\,(transect, new\_front\_crossing)$
      if $dist\left(location_p, location_f\right) > \varepsilon_{past\_front}$ km **then**
        Calculate $transect_p$ **s.t.** $transect_p \perp estimated\_front$
        Command vehicle on $transect_p$
      else
        Continue on current transect
  else if $dist\left(transect\_start, location_p\right) <= transect\_dist_{max}$ **then**
    $valid\_crossings \leftarrow get\_estimation\_crossings(crossings)$
    $estimated\_front \leftarrow linear\_regression\,(valid\_crossings)$
    Calculate $transect_p$ **s.t.** $transect_p \perp estimated\_front$
    Command vehicle on $transect_p$

procedure GET_ESTIMATION_CROSSINGS($crossings$) ▷ First of two options for this procedure
  return Latest front crossing for each vehicle.

procedure GET_ESTIMATION_CROSSINGS($crossings$) ▷ Second of two options for this procedure
  return $\{crossing \in crossings \mid crossing.time > current\_time - \varepsilon_{time}\}$

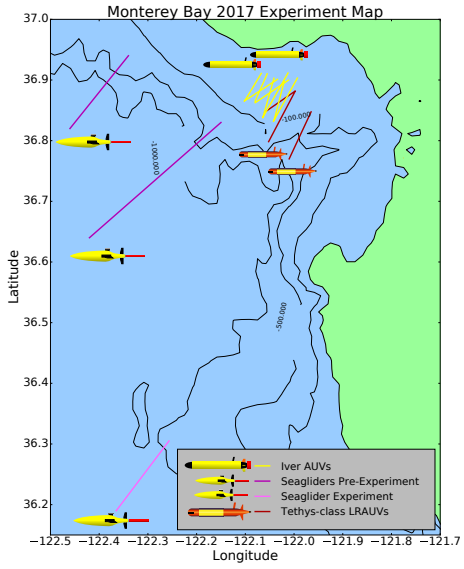

Figure 4: Map of the 2017 pilot experiment region near Monterey Bay, California. The operation regions of the Iver AUVs, Seagliders, and Tethys-class LRAUVs are shown.

GX3-25 and an APS-1540 fluxgate magnetometer. The Iver2 AUVs have an approximate maximum horizontal velocity of 2 m s^{-1} and were operated at a speed of 1.5 m s^{-1} for these trials. These vehicles are shown on board the R/V *Shana Rae* in Figure 5 during operations in August 2016.

Long-Range AUVs Also used in this experiment were two Tethys-Class Long-Range AUVs (Monterey Bay Aquarium Research Institute) [Bellingham et al., 2010; Hobson et al., 2012] (Figure 5). Each vehicle was equipped with a Neil Brown conductivity, temperature, depth (CTD) sensor and a Sea-Bird ECO fluorometer and backscattering sensor. The LRAUVs have an approximate maximum horizontal velocity of 1 m s^{-1} and an endurance of 1,000+ km. The vehicle is capable of sampling to a maximum depth of 200 m in a saw–tooth pattern (i.e. yo-yo). An iridium modem is used for sending commands to the vehicle as well as downloading a subset of the data to the shore. When cellular signal is available, a cellular modem is used to send the full dataset.

Underwater Gliders We used two Seagliders (Kongsberg Underwater Technology, Inc.) [Eriksen et al., 2001] equipped with Seabird SBE3 temperature sensor and SBE4 conductivity sensor, pressure sensor, and Aanderaa 4330F oxygen optode (Figure 5). Sampling occurred approximately every 5 s (0.5 m vertical resolution at typical vertical speeds of 0.1 m s^{-1}). The gliders use a buoyancy engine for propulsion, having an approximate horizontal velocity of 0.25 m s^{-1} and endurance up to 4,600 km. For this experiment, we were tasking the gliders to maximum depths of 600 m (although they are capable of profiling to a maximum depth of 1000 m) in a saw–tooth pattern.

System Architecture

Existing systems are leveraged to deploy a general planning method to a variety of vehicles in a short time frame. The system architecture for all vehicles used in this experiment is shown in Figure 6. The Seaglider and LRAUV both operate remotely using the Iridium network. On each surfacing, GPS, engineering, and scientific data transmits to a shore-based control workstation. This workstation can then issue commands to the vehicle. For this experiment, the planning software ran on a separate shore-based workstation capable of communicating with the workstation controlling the vehicles. In this way it was possible for the planner to receive all the necessary data and send commands to the vehicles in near real-time.

While the Seaglider and LRAUV are nominally able to transmit data and receive new instructions during operations, the Iver AUVs required some modifications to enable these behaviors. Four communication modalities are available to the Iver: Iridium short burst data (SBD), Wi-Fi, 900 MHz RF, and acoustic modem. Scientific data such as position, conductivity, temperature, and timestamps can be received and new commands can be sent over any of these four available communication links. Possible commands include stopping a mission,

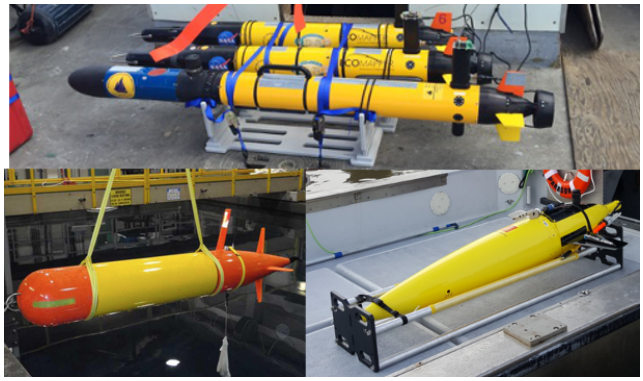

Figure 5: Top: OceanServer Technology, Inc. Iver2 AUVs onboard the R/V *Shana Rae*, Bottom Left: Monterey Bay Aquarium Research Institute's Tethys-Class Long-Range AUV., Bottom Right: Kongsberg Underwater Technology, Inc. Seaglider onboard the R/V *Paragon*

starting a mission already loaded on the vehicle, parking the vehicle and inserting segments of waypoints into the already running mission. Initially, it was planned to use the segment insertion to facilitate the retasking of the vehicles. While these commands were successfully received and interpreted by the vehicle, some unexplained behaviors while using this command precluded its ongoing use. As a temporary work around for the 2017 field trials in Monterey we used the outputs of the planning software to manually program a new mission which was then loaded onto the AUV over the RF link. Due to the short range of the Iver AUVs, a surface vessel remains deployed near the vehicles at all times. This surface vessel also houses the control and planning workstations for the vehicle. The Iridium link was active during this experiment, but was not used for planning purposes.

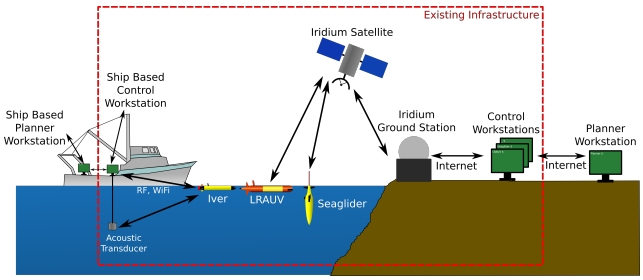

Figure 6: System diagram outlining the communication pathways from the vehicles to the controlling workstations and the planning workstations. The existing infrastructure is outlined with a red dotted line.

Results

An abridged version of the results are presented here. The full results can be found in Branch et al. [2018].

Iver AUV Results

Two Iver AUVs were operated on three days, 4 May, 9 May, and 11 May 2017. They are limited to single day deployments due to the short range of the vehicles. Some operational constraints required modifications to the outlined front tracking control method. The range limitation associated with acoustic and RF communication and the desire to have the ability for quick vehicle recovery required the two Iver AUVs to remain in close proximity to each other. The front tracking algorithm as presented does not guarantee any vehicle synchronization with regards to position. To solve this issue, the vehicles pause at any point in which a new transect could start and waits for every other vehicle to reach their respective decision points. Once all vehicles have paused, the front-crossing detection algorithms are executed for each vehicle. If at least one vehicle has detected a front crossing, a new linear front estimation is generated and all vehicles are commanded orthogonal to it. If no front crossings are detected then all vehicles continue on the current transect.

In this experiment the minimum transect distance was set at 3 km past the current estimated front. The minimum distance required for a vehicle to go past the front-crossing detection on a given transect was set to 0 km, this results in the vehicle turning around at the first decision point after a front crossing is detected. The first decision point can be significantly past the detected front crossing due the minimum transect length. Ideally this would be set to a longer distance to insure that the vehicle has crossed the entire front before calculating a new transect, however due to software constraints for this phase of the deployment this was not possible. Front-geometry estimation was performed with the latest front crossing from each vehicle. The lateral gradient front-crossing detection algorithm was used with the Iver AUVs. Figure 7 shows the results of the Iver experiment on 9 and 11 May, 2017. Two transects were completed per vehicle per day. The starting locations for each vehicle on each day are labeled. Temperature averaged from 10 meters to 15 meters is plotted. All front crossing and front-geometry estimations used during the deployment are shown as blue dots and blue lines respectively. A number of different depth intervals for front-crossing detection were used during the deployment in order to examine the sensitivity of the algorithm. For reference, the front crossings and front-geometry estimations for 10 meter to 15 meter depth range are also plotted in green.

LRAUV Results

The LRAUV experiment took place on 07 May, 2017. Two vehicles, Opah and Tethys, were under the control of the planner and utilized the lateral gradient front-crossing detection method. The minimum transect distance was set at 4.5 km past the current estimated front. The minimum distance required for a vehicle to go past the front-crossing detection on a given transect was set to 0 km, this results in the vehicle turning around at

Underwater Glider Results

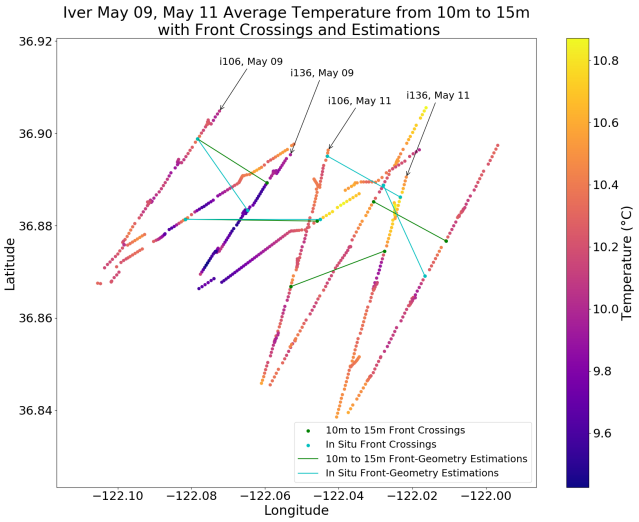

Figure 7: Map view of the temperature averaged from 10 to 15 meters for the Iver transects on 09 and 11 May, 2017. Front crossings and front-geometry estimations used during the experiment are indicated with a blue dot and blue line respectively. Front crossings and front-geometry estimations using data from 10 meters to 15 meters during the experiment are indicated with a green dot and green line respectively. The start location for each vehicle for each day is labeled.

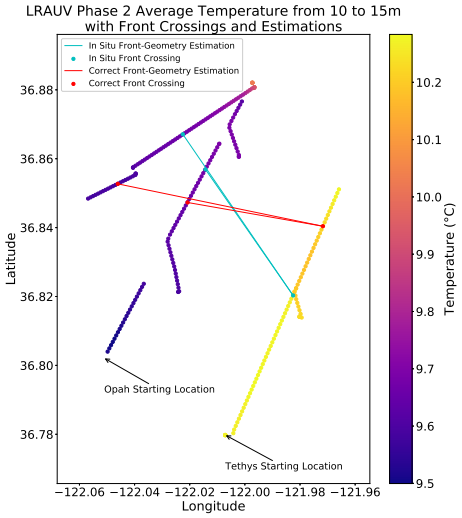

Figure 8: Map view of the temperature averaged from 10 to 15 meters for the LRAUV Phase 2 experiment. The front crossings and front-geometry estimations used in the deployment are plotted as blue dots and blue lines respectively. The correctly calculated front crossing and front-geometry estimations are plotted as red dots and red lines respectively.

the first decision point after a front crossing is detected. Once again, the minimum distance past a front crossing would ideally be larger. Front-geometry estimation was performed with the latest front crossings from each vehicle. Figure 8 shows the results from the phase 2 of the LRAUV experiment. The temperature averaged from 10m to 15m, the interval used for front-crossing detection, is plotted. The algorithm during this period of the deployment ran incorrectly, resulting in erroneous front crossings. The algorithm was re-run correctly in post-processing. Both the front crossings used during the deployment and the correct front crossings are plotted in Figure 8. Opah was able to complete two transect while Tethys only completed one transect due to hardware issues.

Underwater Glider Results

The underwater glider operated off the coast of Point Sur, California from 7 June to 21 June, 2017. From 7 June to 15 June the glider was in a region of strong surface currents, preventing any significant forward movement. The glider transect was relocated and successfully operated from 15 June to 21 June, 2017. During the glider portion of the experiment, only one vehicle was available. Using the method presented here, it is not possible to estimate the orientation of a linear front with a single vehicle. As such, a fixed transect orientation is used in this experiment. The minimum transect distance and the minimum distance to travel past a front were set to a fixed 5 km, independent of the current location of the estimated front. In normal operation these distances would be increased. Due to the short time frame of the experiment these were reduced in order to complete more transects.

A map view of the 6 glider transects plotting the averaged temperature over 10 meters to 15 meters, the interval used for front-crossing detection, can be seen in Figure 9. The front crossings and front estimations are marked with a blue dot and a blue line respectively. The 16 km maximum extent transect is shown in black.

Planning and Execution Challenges

Communication Paradigms The LRAUV and the Seaglider both utilize the Iridium network to enable the off-board planning system to control the vehicle. A centralized off-board planner simplifies vehicle coordination and allows for the use of a variety of vehicles while avoiding unique on-board implementations. This comes at the cost of reduced real time capabilities as vehicles are unable to transmit data and receive new plans during a dive. The default schedule of surfacing activities of the LRAUV and Seaglider also impacts the real time capabilities of the system. Immediately after the data is received from the vehicle, the Iridium connection is closed and the vehicle dives. This induces a one dive delay when using the data from the vehicle for planning purposes. The surfacing schedule can be modified in order to remove this, at the cost of increased

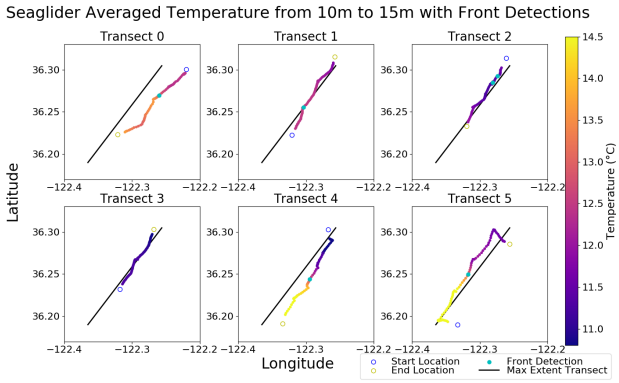

Figure 9: Map view plot of the temperature averaged from 10 to 15 meters for all the glider transects from 15 to 21 June, 2017 off Point Sur, California. Front crossings are indicated with blue dots.

surfacing times.

The Ivers use a similar off-board planning system, however it is ship-based as apposed to shore-based. The range limitations associated with acoustic, RF, and Wi-Fi communication impose additional constraints. It is ideal for the vehicles to be in close proximity so the ship remains in contact with all vehicles simultaneously. Our specific planning approach was modified in order to accommodate this. The real time capabilities could also be improved by utilizing the acoustic communication channel for scientific data and vehicle commanding. Note that the Iridium network is a possible communication modality for the Iver, but was not used during this deployment so the nearby ship could maintain full control of the vehicles.

Data Decimation The bandwidth of the communication channels available is not always large enough to support the transfer of the complete dataset acquired by the vehicle. When this is the case, a subset of the data must be selected for transmission and use by the off-board planner. The Seaglider is capable of sending the full dataset at each surfacing, however the other two vehicles are not. The Iver AUVs selects data at a fixed temporal resolution. The Tethys-Class LRAUV selects data based on the change from the previously transmitted data point. If a given data point differs by a specified amount from the previously selected data point then the given data point is also selected for transmission. During the experiment, we recognized that the decimated dataset from the LRAUV contained large gaps, resulting in suboptimal gridded data. An appropriate data decimation scheme needs to be employed for a given planning method.

Vehicle Safety Vehicle safety concerns must be addressed when implementing a planning system. A concern present with all vehicles is contact with the seafloor. The three vehicles used in the experiment have the capability of autonomously avoiding the seafloor using a sonar based device. However, to increase vehicle endurance, these devices were disabled on the LRAUVs and Seagliders. Instead, an additional layer was added to the planner in order to avoid seafloor collisions. The Seaglider dive depth was altered based on the bathymetry along the expected dive path, while the LRAUV's planned transects were modified to avoid areas with bathymetery less than a specified depth.

A related concern is the lateral position of the vehicles. Each vehicle must remain in the target region. Due to the short experiment periods and limited transect length for the LRAUVs and Ivers, this was not a concern. The Seaglider deployment used boundaries to limit the transect and prevent the vehicle from moving onto the continental shelf. It is also desirable for Ivers to remain in close proximity so the surface ship with the control workstations can be in range of all vehicles simultaneously and quick recoveries are possible. The planning approach was modified to satisfy this constraint.

Related Work

Adaptive sampling and control of multiple autonomous underwater vehicles has been extensively studied, including foundational work with the Autonomous Ocean Sampling Network [Curtin and Bellingham, 2009; Curtin et al., 1993; Haley et al., 2009; Leonard et al., 2007; Ramp et al., 2009]. Much of this work focuses on spatially adapting the control strategy in order to optimally sample a fixed region. The Adaptive Sampling and Prediction project [Leonard et al., 2010] used adaptive control in order to coordinate 6 gliders to fly in loops at fixed spacing. Our method instead performs repeated focused sampling across a single front as it evolves over time.

Other work focused on control strategies that adapt to the current conditions, however not using multi-vehicle coordination. Troesch et al. [2016] uses an ocean model in order to improve the station keeping ability of vertically profiling floats. Eriksen et al. [2001] describes the capabilities of a Seaglider to compensate for drift from currents using depth averaged currents over multiple dives. Those important works focus on adaptive control of vehicles based on current conditions to improve sampling. We instead look at other hydrographic properties in order to optimize sampling of a specific feature.

A number of near real-time feature tracking methods exist for applications such as thermoclines [Cruz and Matos, 2010; Sun et al., 2016; Zhang et al., 2010] and oil spills [Zhang et al., 2011]. These approaches focus on tracking a one-dimensional feature using a single vehicle, while we utilize multiple vehicles to track a two-dimensional feature. Flexas et al. [2018] uses an ocean model and autonomous planning to optimize sampling of submesoscale structures. Our approach focuses on frontal tracking using trailing in-situ vehicle data as apposed to an ocean model.

Other work has investigated two-dimensional feature tracking. Zhang et al. [2013, 2016] utilize the VTHI front detection method on a single vehicle to detect and track an upwelling front on a zig-zag track with a fixed turn angle. Cruz and Matos [2014] tracks any gradient boundary using a single vehicle following a dynamic zig-zag pattern and a lateral gradient detection algorithm to estimate the gradient boundary using an arc whose curvature is defined by the last three front-crossing locations. A similar method can also be applied to tracking the center of a phytoplankton bloom patch [Godin et al., 2011]. Machine learning, in the form of policy learning, has also been applied to the problem of tracking the edge of a harmful algal bloom [Magazzeni et al., 2014]. Other work focuses on tracking algal blooms by flying formations relative to the bloom as tracked by a drifter [Das et al., 2012]. Petillo, Schmidt, and Balasuriya [2012] uses a simulated network of AUVs in order to estimate the boundary of a simulated plume. These all differ from our approach in that we are using multiple vehicles in order to estimate the position and orientation of an ocean front using a method of gridded front detections as well as a linear front model.

Future Work

On-Board Planning

On-board planning can eliminate the constraints imposed by off-board planning. The first option is for all vehicle planning to be performed on-board with all information required for coordination relayed through a centralized off-board server. In the case of our planning method, this would involve sending the front detection locations to a centralized server and sending the front location and orientation to each vehicle from the centralized server. This allows for shorter surfacing windows, use of the full dataset, and real time use of the scientific data. However, less processing power is available for the planning and execution software. An updated front detection method could be required depending on the constraints of on-board processing.

The second option removes the use of a centralized shore-based server for vehicle coordination, instead opting for a peer-to-peer based architecture. This requires a method of inter-vehicle communication such as an acoustic modem, limiting the distance vehicles can be from one another. By performing all planning and execution operations on-board the vehicle, surfacing times can be drastically reduced or the vehicles can operate in areas where surfacing is not always possible, such as an ice-covered environment. Real-time planning and coordination is also possible with this method by removing the need for vehicles to surface for communication. The most appropriate paradigm for planning and execution depends the requirements of the planning method itself.

Front Detection

Throughout this experiment, multiple points of improvement were identified in regards to lateral gradient front detection. Front detection could be improved by gridding data based on distance traveled as opposed to time. This is particularly important for slower moving vehicles such as underwater gliders. The gridding process itself could also be improved by using objective mapping. In this experiment temperature was used, other ocean properties such as, buoyancy could also be used. The lateral gradient front detection method consists of many parameters, a more in-depth analysis of the effects of these parameters would be beneficial. Our front-crossing detection technique could be extended in order to select a crossing based on a set of criteria such as front direction (i.e. cold-to-warm versus warm-to-cold), gradient strength, and front size. By using these different properties a specific front can be targeted.

Conclusion

This work presents a planning and execution system for a heterogeneous fleet of underwater vehicles and demonstrates it with a method of adaptive control using multiple autonomous underwater vehicles in order to track an ocean front evolving over time. This method utilizes an off-board planner for near real-time front detection, ocean front estimation using a linear model, and vehicle retasking. We build upon the prior efforts of the AOSN deployments and takes a further step towards a fully-autonomous adaptive sampling framework [Thompson et al., 2017].

The experiment was conducted in May and June, 2017 in and around Monterey Bay, California. Three types vehicles were used, two Tethys-Class Long-Range AUVs, two short-range Iver AUVs, and one autonomous underwater glider, a Seaglider. During this experiment we demonstrated the performance of the lateral gradient front detection method on data from all three vehicles and the capability of the autonomous control method for front tracking. We showed that this method is both suitable for a multi-vehicle approach with a dynamic front position and orientation and a single-vehicle approach utilizing a fixed front orientation. The multi-vehicle approach allows for improved synopticity over a zig-zag method when sampling a front. While the use of off-board planning algorithms provides more processing power and allows for flexible implementation for different platforms.

Acknowledgments The following work was done under the framework of the Keck Institute for Space Studies (KISS)-funded project "Science-driven Autonomous and Heterogeneous Robotic Networks: A Vision for Future Ocean Observations"[Thompson et al., 2017]. Portions of this work were funded by the Keck Institute and Woods Hole Oceanographic Institution. Portions of this work were performed by the Jet Propulsion Laboratory, California Institute of Technology, under contract with the National Aeronautics and Space Administration.

References

Bellingham, J. G.; Zhang, Y.; Kerwin, J. E.; Erikson, J.; Hobson, B.; Kieft, B.; Godin, M.; McEwen, R.; Hoover, T.; Paul, J.; et al. 2010. Efficient propulsion for the tethys long-range autonomous underwater vehicle. In *Autonomous Underwater Vehicles (AUV), 2010 IEEE/OES*, 1–7. IEEE.

Branch, A.; Flexas, M. M.; Claus, B.; Clark, E. B.; Thompson, A. F.; Chien, S.; Kinsey, J. C.; Fratantoni, D. M.; Zhang, Y.; Kieft, B.; Hobson, B.; and Chavez, F. P. 2018. Front delineation and tracking with multiple underwater vehicles. *J. Field Robotics* in review.

Crowell, J. 2006. Small auv for hydrographic applications. In *OCEANS 2006*, 1–6.

Cruz, N. A., and Matos, A. C. 2010. Adaptive sampling of thermoclines with autonomous underwater vehicles. In *OCEANS 2010*, 1–6. IEEE.

Cruz, N. A., and Matos, A. C. 2014. Autonomous tracking of a horizontal boundary. In *Oceans-St. John's, 2014*, 1–6. IEEE.

Curtin, T. B., and Bellingham, J. G. 2009. Progress toward autonomous ocean sampling networks. *Deep Sea Research Part II: Topical Studies in Oceanography* 56(3):62 – 67. AOSN II: The Science and Technology of an Autonomous Ocean Sampling Network.

Curtin, T. B.; Bellingham, J. G.; Catipovic, J.; and Webb, D. 1993. Autonomous oceanographic sampling networks. *Oceanography* 6(3):86–94.

Das, J.; Py, F.; Maughan, T.; OReilly, T.; Messié, M.; Ryan, J.; Sukhatme, G. S.; and Rajan, K. 2012. Coordinated sampling of dynamic oceanographic features with underwater vehicles and drifters. *The International Journal of Robotics Research* 31(5):626–646.

Eriksen, C. C.; Osse, T. J.; Light, R. D.; Wen, T.; Lehman, T. W.; Sabin, P. L.; Ballard, J. W.; and Chiodi, A. M. 2001. Seaglider: A long-range autonomous underwater vehicle for oceanographic research. *IEEE J. Oceanic Eng.* 26:424436.

Flexas, M. M.; Troesch, M. I.; Chien, S.; Thompson, A. F.; Chu, S.; Branch, A.; Farrara, J. D.; and Chao, Y. 2018. Autonomous sampling of ocean submesoscale fronts with ocean gliders and numerical model forecasting. *Journal of Atmospheric and Oceanic Technology* 35(3):503–521.

Godin, M. A.; Zhang, Y.; Ryan, J. P.; Hoover, T. T.; and Bellingham, J. G. 2011. Phytoplankton bloom patch center localization by the tethys autonomous underwater vehicle. In *OCEANS'11 MTS/IEEE KONA*, 1–6.

Haley, P.; Lermusiaux, P.; Robinson, A.; Leslie, W.; Logoutov, O.; Cossarini, G.; Liang, X.; Moreno, P.; Ramp, S.; Doyle, J.; Bellingham, J.; Chavez, F.; and Johnston, S. 2009. Forecasting and reanalysis in the monterey bay/california current region for the autonomous ocean sampling network-ii experiment. *Deep Sea Research Part II: Topical Studies in Oceanography* 56(3):127 – 148. AOSN II: The Science and Technology of an Autonomous Ocean Sampling Network.

Hickey, B. M. 1979. The california current system-hypotheses and facts. *Prog. Oceanogr.* 8:191–279.

Hobson, B. W.; Bellingham, J. G.; Kieft, B.; McEwen, R.; Godin, M.; and Zhang, Y. 2012. Tethys-class long range auvs-extending the endurance of propeller-driven cruising auvs from days to weeks. In *Autonomous Underwater Vehicles (AUV), 2012 IEEE/OES*, 1–8. IEEE.

Leonard, N. E.; Paley, D. A.; Lekien, F.; Sepulchre, R.; Fratantoni, D. M.; and Davis, R. E. 2007. Collective motion, sensor networks, and ocean sampling. *Proceedings of the IEEE* 95(1):48–74.

Leonard, N. E.; Paley, D. A.; Davis, R. E.; Fratantoni, D. M.; Lekien, F.; and Zhang, F. 2010. Coordinated control of an underwater glider fleet in an adaptive ocean sampling field experiment in monterey bay. *Journal of Field Robotics* 27(6):718–740.

Lynn, R. J., and Simpson, J. J. 1987. The california current system: The seasonal variability of its physical characteristics. *J. Geophys. Res.* 92:12947–12966.

Magazzeni, D.; Py, F.; Fox, M.; Long, D.; and Rajan, K. 2014. Policy learning for autonomous feature tracking. *Autonomous Robots* 37(1):47–69.

Molemaker, M. J.; McWilliams, J. C.; and Dewar, W. K. 2015. Submesoscale instability and generation of mesoscale anticyclones near a separation of the california undercurrent. *J. Phys. Oc.* 45:613–629.

Monterey Bay Aquarium Research Institute. 2017. Canon spring 2017 expedition.

Petillo, S.; Schmidt, H.; and Balasuriya, A. 2012. Constructing a distributed auv network for underwater plume-tracking operations. *International Journal of Distributed Sensor Networks* 2012:Article ID 191235, 12pp.

Ramp, S.; Davis, R.; Leonard, N.; Shulman, I.; Chao, Y.; Robinson, A.; Marsden, J.; Lermusiaux, P.; Fratantoni, D.; Paduan, J.; Chavez, F.; Bahr, F.; Liang, S.; Leslie, W.; and Li, Z. 2009. Preparing to predict: The second autonomous ocean sampling network (aosn-ii) experiment in the monterey bay. *Deep Sea Research Part II: Topical Studies in Oceanography* 56(3):68 – 86. AOSN II: The Science and Technology of an Autonomous Ocean Sampling Network.

Sun, L.; Li, Y.; Yan, S.; Wang, J.; and Chen, Z. 2016. Thermocline tracking using a portable autonomous underwater vehicle based on adaptive threshold. In *OCEANS 2016-Shanghai*, 1–4. IEEE.

REFERENCES

Thompson, A. F.; Chao, Y.; Chien, S.; Kinsey, J.; Flexas, M. M.; Erickson, Z. K.; Farrara, J.; Fratantoni, D.; Branch, A.; Chu, S.; Troesch, M.; Claus, B.; and Kepper, J. 2017. Satellites to seafloor: Toward fully autonomous ocean sampling. *Oceanography* 30(2):160–168.

Troesch, M.; Chien, S. A.; Chao, Y.; and Farrara, J. D. 2016. Planning and control of marine floats in the presence of dynamic, uncertain currents. In *International Conference on Automated Planning and Scheduling*, 431–440.

Zhang, Y.; Bellingham, J. G.; Godin, M.; Ryan, J. P.; McEwen, R. S.; Kieft, B.; Hobson, B.; and Hoover, T. 2010. Thermocline tracking based on peak-gradient detection by an autonomous underwater vehicle. In *OCEANS 2010*, 1–4. IEEE.

Zhang, Y.; McEwen, R. S.; Ryan, J. P.; Bellingham, J. G.; Thomas, H.; Thompson, C. H.; and Rienecker, E. 2011. A peak-capture algorithm used on an autonomous underwater vehicle in the 2010 gulf of mexico oil spill response scientific survey. *Journal of Field Robotics* 28(4):484–496.

Zhang, Y.; Bellingham, J. G.; Ryan, J. P.; Kieft, B.; and Stanway, M. J. 2013. Two-dimensional mapping and tracking of a coastal upwelling front by an autonomous underwater vehicle. *Proc. MTS/IEEE Oceans'13* 1–4.

Zhang, Y.; Bellingham, J. G.; Ryan, J. P.; Kieft, B.; and Stanway, M. J. 2016. Autonomous four-dimensional mapping and tracking of a coastal upwelling front by an autonomous underwater vehicle. *Journal of Field Robotics* 33(1):67–81.